**ICAST 2017: 28th International Conference on Adaptive Structures and Technologies**
**October 8-11, 2017, Cracow, Poland**

# Progress on the Design, Analysis and Experimental Testing of a Composite Fish Bone Active Camber Morphing Wing

Andres E Rivero [1,*], Paul M Weaver [1,2], Jonathan E Cooper [3], Benjamin KS Woods [1]

[1] *ACCIS, Department of Aerospace Engineering, University of Bristol, Bristol, UK*
[2] Bernal Institute in Composite Materials and Structures, University of Limerick, Limerick, Ireland
[3] Department of Aerospace Engineering, University of Bristol, Bristol, UK

## Abstract

This work presents progress on the design, analysis and manufacture of the first composite Fish Bone Active Camber (FishBAC) morphing wing. The FishBAC is a morphing trailing edge device that is able to generate large, smooth and continuous changes in aerofoil camber distribution from a biologically inspired compliant structure. It has already shown promising results in terms of its large lift control authority and its ability to generate significantly lower drag when compared to the traditional trailing edge flaps, which are ubiquitous in aviation. However, prototypes to date have been manufactured using 3D printed isotropic materials (i.e. polymers), and they were designed around a one-dimensional structural model using Euler-Bernoulli Beam Theory. As a consequence, existing prototypes are unable to take advantage of the significant aerodynamic and structural benefits that can be achieved with material anisotropy and spanwise varying deformations. The focus of this work is on designing, manufacturing and testing the first composite FishBAC device. The design was performed using a recently developed two-dimensional discontinuous Kirchhoff-Love plate model, where fully anisotropic laminates can be analysed and static displacement fields can be predicted under transverse pressure loads and actuation inputs. This model has been validated using FEM, but no experimental comparisons have been performed due to the lack of a composite FishBAC prototype. A 'modular' design approach was followed for the wind tunnel model, which allows for easy installation and removal of both the leading edge and composite FishBACs devices from the main load bearing member of the wing. This gives the option to manufacture several FishBACs with different material parameters (i.e. stacking sequences) and structural configurations, as well as modifying the leading edge, if other morphing concepts are to be tested.

## 1. INTRODUCTION

Conventional fixed-wing aircraft are controlled by varying the amount of forces and moments that the wings generate. These changes in forces are generated by variations in the camber distribution of the aerofoils, which are achieved by actuating a series of hinged panels commonly known as trailing edge plain flaps. Depending on the location of each one of these panels, they received the names of elevators (pitch control), rudder (yaw), ailerons (roll) or trailing edge flap (high-lift device).

Although effective in providing control authority, hinged plain flaps are a source of drag (and subsequently of noise) due to the sharp and discontinuous change in camber. An alternative to using hinged plain flaps is to continuously varying the camber distribution by having a wing that is able to 'morph' into different geometric configurations. Variable camber morphing devices can provide similar lift control authority (i.e. $\Delta C_L$) for lower drag, resulting in higher lift-to-drag ratio for a broader range of angles of attack. Furthermore, if the morphing device allows for spanwise variations in camber distribution, it can be used to optimise the spanwise lift distribution, potentially reducing the induced drag [1].

*andres.riverobracho@bristol.ac.uk

In fact, variable camber morphing is not a new concept. One of the first designs that implemented this approach was introduced in 1920 by H.F. Parker, where a 'rib springs' mechanism was capable of inducing changes in camber [2]. Furthermore, several variable camber patents were filed during 1930 and 1940 [3, 4, 5]. Unfortunately, a common aspect among these four concepts is that they all involved the use of heavy and complex actuation mechanisms that ended up adding significant structural weight. Because of this, the interest in camber morphing (and morphing aircraft in general) was lost during those initial decades.

Due to advances in lightweight and smart structures and materials, morphing aircraft have become a popular subject of study since the beginning of the 21st century. Significant research outputs have been generated in the subject of variable camber morphing, and they are summarised by Thill et al. [6] and Barbarino et al. [7]. The main objective of these 'new' concepts was to address the weight and complexity penalties of 'traditional' morphing mechanisms, so that the real benefits can be observed.

One of these first 'new' designs is the DARPA Smart Wing [8], where a centre laminate with honeycomb core and silicone skin give the trailing edge the flexibility needed to create changes in camber. Furthermore, some research groups have studied variable camber using leading edge devices, including a compliant "droop-nose" morphing leading edge using superelastic materials [9], a both compliant-based leading and trailing edge mechanisms [10]. Furthermore, other concepts achieved variable camber by focusing the camber changes on the trailing edge, for example, by embedding actuators within the wing skin [11, 12], exploiting bistability in non-symmetrical fibre-reinforced composite laminates [13, 14] and also by active actuation of the internal load bearing structural members [15, 16, 17, 18].

Moreover, the NASA-Boeing VCCTEF [19] investigated variable camber morphing with spanwise variations by using a series of panels that were individually hinged to each other, providing significantly higher degrees of freedom than a traditional plain flap. Even though this concept successfully showed the potential aerodynamic benefits of exploiting camber morphing along the span, the design adds significantly structural complexity to the wing. Similarly, Flexsys Flexfoil [20] morphing device is capable of generating limited camber variations along the span, however, at the expense of spanwise rigidity.

An alternative to these concepts is the Fish Bone Active Camber (FishBAC) morphing trailing edge device [21], which consists of a central plate (spine) that acts as the main load bearing member and it is actively actuated by a set of tendons that transmit the actuating loads to the morphing device. Furthermore, a series of spanwise stringers provide localised structural rigidity along the span without adding significant chordwise stiffness (Figure 1). This allows to focus deformations in the desire camber distribution, while simultaneously controlling the deflections in the spanwise direction due to aerodynamic loads. Since the actuating loads are locally transmitted by tendons, large variations in camber distribution can be achieved, along the span, by having multiple actuating points. Having this deflection 'control' gives the FishBAC the ability to potentially optimise spanwise lift distributions, not only reducing the profile drag of the aerofoil (compared to a plain flap), but also reducing the induced drag.

The initial design and analysis of this concept was performed using an analytical model based on Euler-Bernoulli beam model [22], while the first prototypes were 3D-printed using Acrylonitrile Butadiene Styrene (ABS) plastic. However, a beam model is not able to evaluate a three-dimensional pressure distributions (i.e. distributed loads with chordwise and spanwise variations) and spanwise variation in deflections, nor handling composite laminates. Furthermore, in order to feasibly use the FishBAC in

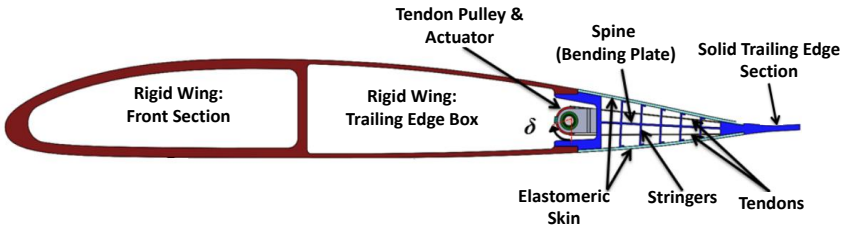


**Figure 1.** Schematic of the structural configuration of the Fish Bone Active Camber morphing trailing edge concept [22]

realistic applications, a lightweight material stronger and stiffer material than ABS plastic must be used. As consequence, designing and manufacturing a FishBAC with a composite spine is vital. Using composite laminates not only increases the robustness of the morphing device, but also expands the design space for stiffness tailoring.

In response to these needs, a parametric discontinuous Kirchhoff-Love plate model of the FishBAC was developed as a design tool. The model is capable of capturing the in-plane and out-of-plane displacement due to both aerodynamic pressure (i.e. transverse loading distribution) and actuation loads (i.e. point moments at the trailing edge), while accounting for stiffness discontinuities due to stringers, using a single system of linear equations. The scope of this effort represents a significant advance beyond existing analytical plate models for discontinuous structures in the literature (for any structure) and a significantly more capable approach to modelling the FishBAC. The analytical nature of the model not only allows local stiffness properties to be defined for each individual plate 'partition', but also to rapidly modify the geometric parameters (e.g. stringer spacing, spine and skin thickness, wing dimensions, among others) and material properties. Lastly, unlike Finite Element Method (FEM), the analytical model is 'mesh-independent', which means that its convergence only depends on the number of the assumed shape functions that are used.

In order to experimentally validate the structural model and to further study the aerodynamics of variable camber morphing, a wind tunnel model of a composite spine FishBAC has been designed and it is currently being manufactured. To achieve a feasible spine design, a combination of the developed plate model is being used together with a one-dimensional fluid-structure interaction model that has been previously developed [23].

## 2. Analytical Model

The following section introduces the fundamentals of plate theory that are used to model the behaviour of the FishBAC, as well as the specific procedure that is followed to obtain the displacement fields, including an introduction to the Rayleigh-Ritz method for structural analysis.

The Rayleigh-Ritz Method is a variational method that can be used to approximate solutions to partial differential equations based on energy formulations. Its foundation lies in the principle of conservation of total energy in a closed system. For an initially flat plate, these energy formulations can be written in terms of a total energy expression that is a function of the plate displacement's $u^o, v^o$ and $w$ (Equation 1), where $U$ refers to the strain energy of the body, $V$ and $W$ are the potential energies due to transverse and in-plane loads, respectively, and $T$ is the kinetic energy.

$$\Pi(u^o, v^o, w) = U + W + V - T = \text{constant} \tag{1}$$

### 2.1 Strain Energy

From a mechanics point of view, this implies that the sum of the strain energy of the body and the kinetic and potential energies due to external loads is a stationary value (in absence of friction within the structure) [24]. For an elastic body, the total strain energy is defined as the integral of the sum of the products of stresses and strains across the volume of the body Equation 2:

$$U = \frac{1}{2}\iiint(\sigma_x\epsilon_x + \sigma_y\epsilon_y + \sigma_z\epsilon_z + \sigma_{xz}\epsilon_{xz} + \sigma_{yz}\epsilon_{yz} + \sigma_{xy}\epsilon_{xy})dxdydz\,. \tag{2}$$

As mentioned earlier, the presented analytical model is based on Kirchhoff-Love plate theory. Therefore, through-thickness and transverse shear strains are neglected (i.e. $\epsilon_z = \epsilon_{xz} = \epsilon_{yz} = 0$), as stated by [24]. Furthermore, the in-plane strains of the laminate can be obtained in terms of the plate's displacement, which leads to a mathematical expression in function of the plate's displacements and its derivatives (Equation 3): and the stiffness terms, which in this case are expressed in terms of the $ABD$ Matrix, when Classical Laminate Theory (CLT) is implemented. The $ABD$ Matrix describes the stiffness of the composite laminate; it combines both material and geometric stiffness in a single expression [25].

$$\epsilon_x = \frac{\partial u^o}{\partial x} - z\frac{\partial^2 w}{\partial x^2} \qquad \epsilon_y = \frac{\partial v^o}{\partial y} - z\frac{\partial^2 w}{\partial y^2} \qquad \epsilon_{xy} = \frac{\partial u^o}{\partial y} + \frac{\partial v^o}{\partial x} - 2z\frac{\partial^2 w}{\partial x \partial y}\,. \tag{3}$$

### 2.2 Potential Energy: External Loads

The net aerodynamic pressure distribution acting on the FishBAC (which is found separately using an aerodynamic solver, e.g. panel methods or CFD) can be treated as a transverse pressure distribution, on the plate, with both variations in $x$ and $y$. The potential energy due to transverse pressure distributions (i.e. force per unit area) is defined as the integral of the pressure times the transverse displacement across the surface area (Equation 4) [24]. The potential energy due to the actuation moments at the trailing edge depends on the first derivative of the transverse displacement along the bending direction and the applied moment intensity $M_x$ (Equation 5) [26].

$$V_{ij} = -\iint q(x,y)\, w(x,y)\, dx\, dy \tag{4}$$

$$W_{ij} = -\int M_x \frac{\partial w(a_i, y)}{\partial x}\, dy \tag{5}$$

### 2.3 Shape Functions and Energy Minimisation

Within the context of Rayleigh-Ritz method, all three displacements (i.e. $u^o$, $v^o$ and $w$) are normally defined in the form of three sets of double summations of terms in the $x$- and $y$-direction that satisfy compatibility conditions, each set containing a known and assumed displacement field, scaled by an unknown amplitude. Since the structural dimensions and material stiffness are known, these displacement amplitudes become the unknowns in the mathematical model.

From the mechanics point of view, orthogonal polynomials are commonly used to capture structural deflections when localised features occur, such as in anisotropic composite laminates. For example, Legendre polynomials have been successfully implemented in several variable stiffness beam and plate analysis [27, 28, 29], however, their integrals have an exact value of zero when integrated across their normalised domain. This would imply that there is zero net work when a uniform transverse pressure distribution and external moments are applied (Equations 4 and 5). On the other hand, Chebyshev polynomials do not present this property. Therefore, the shape functions that are implemented in this analytical model are Chebyshev Polynomials of the First Kind, defined as (Equation 6):

$$T(\zeta) = \frac{1}{2}\left[\left(\zeta - \sqrt{\zeta^2 - 1}\right)^n + \left(\zeta + \sqrt{\zeta^2 - 1}\right)^n\right]. \tag{6}$$

As previously stated, the Rayleigh-Ritz method is based on the assumption of conservation of total energy in a closed system. Therefore, differentiating the total energy formulation with respect to any of the unknown constant shape function amplitudes (e.g. $Q_{mn}$, $R_{mn}$ and $S_{mn}$) leads to a state of minimum energy (Equation 7)[30, 31]. This approach is computationally convenient, as the static behaviour of the highly discontinuous geometry can be captured with a single coefficient matrix.

$$\frac{\partial \Pi}{\partial Q^{ij}_{mn}}, \frac{\partial \Pi}{\partial R^{ij}_{mn}}, \frac{\partial \Pi}{\partial S^{ij}_{mn}} = 0 \qquad \begin{cases} m = 1, 2, ..., M \\ n = 1, 2, ..., N \end{cases} \tag{7}$$

### 2.4 Stiffness Discontinuities

The stiffness of the FishBAC is inherently discontinuous due to the presence of the stringers, which implies that the energy balance presented in Equation 1 must be calculated in each section of uniform stiffness as the $ABD$ Matrix terms vary significantly between regions with and without stringers.

In structures with stiffness discontinuities, shear force and bending moments at each 'joint' must be continuous when approached from either side of the boundary. Since Chebyshev polynomials do not inherently meet this type of structural continuity at local boundaries, these have to be enforced by other means. There are two common approaches for ensuring displacement and rotation continuities: Lagrangre Multiplier Method or Courant's Penalty Method [30, 31]. Due to the number of equations and separate Lagrange Multipliers that would need to be solved for in this application, the Courant's Penalty Method in form of spring penalty energies is used.

### 2.5 Courant's Penalty Method

As mentioned in the previous subsection, each one of the plates sections is assumed to be joined with an artificial penalty spring with a stiffness equal to $k_k$. Given the relevant degrees of freedom between partitions in this analysis, a set of penalty equations for the three displacements $u^0, v^0$ and $w$ and two out-of-plane rotations $\partial w/\partial x$ and $\partial w/\partial y$ are defined (see Equation 8 for example). When the spring stiffness $k_k$ is 'large', the energy is minimised when the difference in displacements and rotations in are minimal. Convergence studies (against FEM model) for selecting the magnitude of both chordwise and spanwise penalty springs were performed using the FishBAC's geometry. These studies showed that, for four different spine composite ply stacking sequences, a value of $k_k = 1 \times 10^8$ N/m provides stable results.

$$U_{pu,kl} = \frac{k_k}{2} \int_{-b_j/2}^{b_j/2} (u_k(x_{kl}^{(+)}, y_j) - u_l(x_{kl}^{(-)}, y_j))^2 dy \tag{8a}$$

$$U_{pw_x,kl} = \frac{k_k}{2} \int_{-b_j/2}^{b_j/2} \left( \frac{\partial w_k(x_{kl}^{(+)}, y_j)}{\partial x} - \frac{\partial w_l(x_{kl}^{(-)}, y_j)}{\partial x} \right)^2 dy \tag{8b}$$

## 3. Composite Wind Tunnel Prototype

A two-dimensional wind tunnel test model was designed using a NACA 23012 aerofoil profile, with a chord length of 270 mm and span of 1000 mm. The chordwise dimension was chosen based on a full-size MBB Bo 105 helicopter rotor blade [32], while the span was chosen based on the wall-to-wall dimensions of Swansea University's subsonic wind tunnel to provide as close to two-dimensional flow as possible.

The design concept consists of a modular wing, where both the leading and trailing edge can be detached from a box spar. This not only allows to install different FishBAC configurations, but also to install a trailing edge flap. Furthermore, it can be used by other researchers to test morphing leading edge concepts. A combination of 3D-printed "ABS like" plastic, Aluminium 6082T and High-Strength Carbon Fibre prepreg are used to manufacture this prototype. Lastly, the wind tunnel model is designed for testing over a range of flow velocities up to a maximum of 50 m/s. Under these conditions, a Reynolds number of greater than 1 million will be achieved.

### 3.1 Preliminary Estimates

The sizing of the FishBAC morphing device is driven by the thickness and material stiffness of the spine, which drives the maximum deflection of the FishBAC achievable for a given actuation system. A target maximum deflection of $y/c = 0.1$ (i.e. 27 mm, in this case) was chosen based on previous aerodynamic analysis to provide a high lift control authority. Consequently, the spine thickness and material layup is selected to achieve this target deflection. An intermediate modulus Carbon Fibre prepreg (Hexcel® 8552/IM7) has been selected as the spine's material. For ease of manufacturing, it was decided to restrict the ply angle orientation to cross-ply configurations (i.e. $0^\circ$ or $90^\circ$ plies). A two-step analysis was performed: first, the analytical model was run under actuation loads, followed by superimposing the aerodynamic pressure distribution obtained using an existing fluid-structure interaction model [23] with the new two-dimensional plate model.

#### 3.1.1 Actuation Loads Without Aerodynamics

The first estimation consisted of a comparison of static deflections, in absence of aerodynamic loads, between the one-dimensional Euler-Bernoulli beam model and the two-dimensional Kirchhoff-Love plate model. This not only allows to have an estimate of the actuation requirements, but also allows to compare the performance of the

two models. The material properties of the carbon fibre prepreg, skin and 3D-printed plastic that were used are presented in Table 1.

In order to create a high stiffness anisotropy between chordwise (low) and spanwise (high) stiffness, an initial spine layup of $[90/0/90]_S$ (where $0°$ is aligned with the chordwise direction) was analysed. However, this resulted in an actuation torque requirement of at least $6.5\,\mathrm{N}\cdot\mathrm{m}$ (neglecting friction in the actuation mechanism). Considering the size of the aerofoil, there are no off-the-shelf actuators that could provide the require torque that can fit inside the aerofoil dimensions.

Based on these preliminary estimates, it was considered that reducing the spine thickness was the most feasible option to reduce the actuation requirements. In order to achieve this, the spine thickness was reduced in half by having a layup of $[90/0/90]_T$, which is also more compliant from the material stiffness point of view than the $[90/0/90]_S$ layup.

A positive and negative moment input sweep was performed to compare both structural models in absence of aerodynamic loads. Since the beam model is not capable of analysing composite laminates, an effective Young's modulus in the chordwise direction is calculated as (Equation 9):

$$E_x^b = \frac{12}{d_{11}\cdot t^3} \quad , \tag{9}$$

where $d_{11}$ is obtained by calculating the inverse of the ABD Matrix using Classical Laminate Theory (CLT).

Results show that the one-dimensional beam model and two-dimensional plate model agree within 14% with each other (Figure 2), when comparing the average edge displacements. Note that this percentage difference corresponds to the average error along the spanwise free edge, and consequently, this may be significantly affected by localised edge features. This means that the 14% discrepancy is expected to be the largest value, as the average percentage difference across the entire surface is expected to be lower. The main discrepancy between the two models is the differences in spanwise displacement: the plate model observes significant variations along the span, while the beam model is only able to predict a uniform displacement due to its one-dimensional formulation. These results highlight the need of a two-dimensional structural formulation to analyse and further optimise the Fish Bone Active Camber Morphing concept.

Also, results show that deflections of approximate 8% chord can be obtained by applying a total moment input of approximately $2.84\,\mathrm{N}\cdot\mathrm{m}$, which is achievable with off-the-shelf actuators. Details on the actuator selection will be addressed in the next subsection.

### 3.1.2 Deflections Under Aerodynamic Loads

There are two key factors that need to be considered when a morphing device is subject to a freestream flow: the actuation requirements vary due to the presence of aerodynamic forces and moments and, as a consequence, the actuation requirements to induce certain camber deformations are no longer equal to the ones calculated without aerodynamic loads. Since the aerodynamic loads very with varying camber distribution, the structural and aerodynamic analysis cannot be performed independently, as they affect each other. Consequently, fluid-structure interaction (FSI) routines are implemented to properly model compliant structures under fluid flows.

Even though the fluid-structure interaction model for the two-dimensional plate model is yet to be developed, aerodynamic pressure distributions from the one-dimensional FSI [23] can be extracted and applied to the plate model. Since the one-dimensional model cannot capture spanwise variations in deflection, spanwise pressure uniformity must be assumed. This will not allow to capture any aerodynamic changes due to asymmetric moment inputs, however, it is a good estimation for symmetric actuation inputs, considering that the wind tunnel model will be used for a two-dimensional wind tunnel test, where spanwise lift distribution is expected to be "fairly" uniform.

A freestream flow velocity of Mach 0.15 (i.e. $50\,\mathrm{m/s}$ at room temperature), and an angle of attack of $5°$ are used to obtain pressure distributions. These correspond to the maximum speed that can be achieved in the wind

**Table 1.** Material properties of CFRP, ABS and Silicone [23, 33]. Note that the shear modulus of both ABS and Silicone are obtained using the isotropic Young's modulus and Poisson's ratio.

| Material | CFRP | ABS | Silicone |
|---|---|---|---|
| $E_{11}$ | 161 GPa | 2.9 GPa | 3.18 MPa |
| $E_{22}$ | 11.4 GPa | | |
| $G_{12}$ | 5.17 GPa | N/A | N/A |
| $\nu_{12}$ | 0.34 | 0.35 | 0.425 |
| $t$ | 0.125 mm | N/A | N/A |

tunnel and the maximum aerodynamic pressure distribution that the FishBAC will experience, respectively. Ten different moment inputs were applied, with their respective aerodynamic pressure distributions. Figure 3 shows the results under aerodynamic loads.

Results show that the two-dimensional plate and one-dimensional beam models agree within an average error of 15%, when displacement percentage difference is calculated along the spanwise free edge. As mentioned earlier, the main source of error is also the spanwise variation in displacement that the plate model captures, which are mainly due applying the actuation loads discretely in the plate model, versus applying it uniformly in the beam model.

Furthermore, it is observed that the actuation requirements to generate a tip deflection between 8% and 10% chord increased by approximately 50%. As mentioned earlier, even though the two-dimensional plate model is not coupled with aerodynamic loads, these results are meaningful as the pressure distributions that were applied were obtained from an already converged fluid-structure interaction model. Lastly, these results show that a spine thickness of $0.375\,\mathrm{mm}$, with a stacking sequence of $[90/0/90]$ is suitable for the composite wind tunnel model, and will be able to achieve the targeted chord deflections of 8-10%.

### 3.2 Detailed Design and Manufacture

This subsection introduces details on the design and manufacture of the wind tunnel model, including design features and actuator selection. Furthermore, it describes the current and future manufacturing process.

#### 3.2.1 Design Features & Actuator Selection

As mentioned earlier, a modular approach is implemented in the wind tunnel model design. This allows for detachable leading and trailing edge, allowing for testing multiple leading and trailing edge devices, including the FishBAC or a plain trailing edge flap. A $19.05 \times 19.05 \times 3.25$ mm stainless steel box spar acts as the main load bearing member of the wing. The leading edge is mounted to a $15.88 \times 6.25$ mm stainless steel, which is also mounted to the box spar. Furthermore, the actuators are mounted to a removable trailing edge clamp, which is itself attached to the main wing by a series of transverse screws. Moreover, the FishBAC device is clamped to the removable trailing edge clamp by also using a series of transverse screws. Lastly, a series of spanwise oriented carbon fibre pultruded tubes are added, in nine various locations, to both increase the torsional and spanwise stiffness of the non-morphing portion of the wing. Figure 4 shows a profile view of the wind tunnel model.

Based on the results shown in Figures 2 and 3 and the dimensions of the aerofoil, the actuation selection was performed. In this design, the driving factor was the aerofoil dimensions. Because of their small size ($35.5 \times 30 \times 10$ mm), the KST X10 wing servo actuator was selected [34]. However, since each one of these actuators produce a maximum torque of $1.05\,\mathrm{N \cdot m}$ when running at maximum voltage, two actuators per tendon are needed to achieve the required actuation energy, considering that frictional losses are currently being neglected in both analytical structural models.

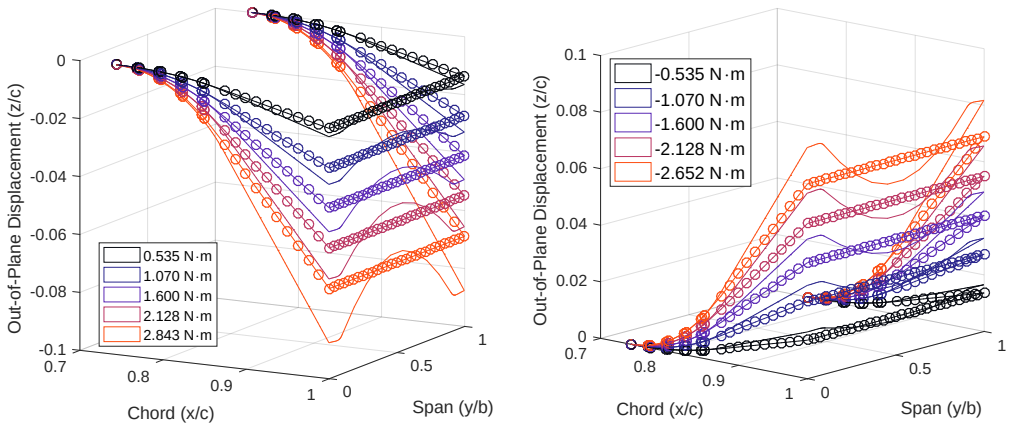


**Figure 2.** Two-dimensional plate model (solid) vs. one-dimensional beam model (○) actuation moment sweep in absence of aerodynamic loads. Moments correspond to total moment input.

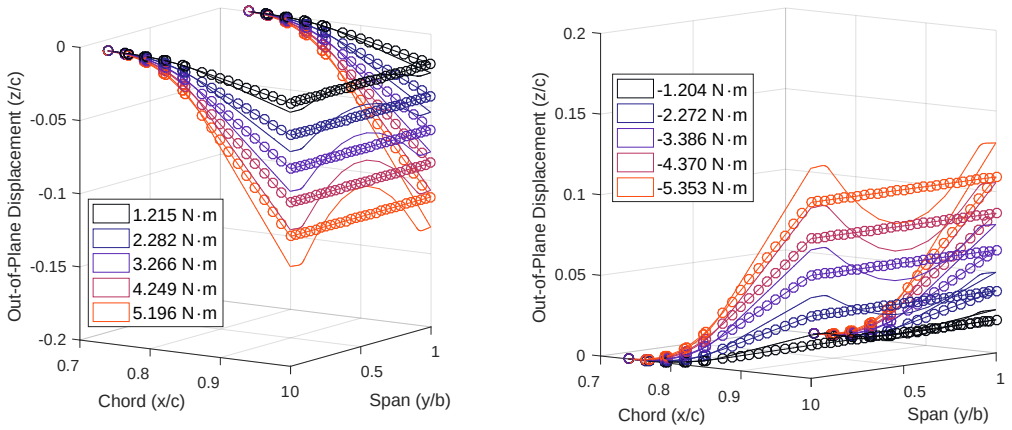


**Figure 3.** Two-dimensional plate model (solid) vs. one-dimensional beam model (○) actuation moment sweep under a freestream flow of Mach number of M = 0.15 and 5° angle of attack. Moments correspond to total moment input.

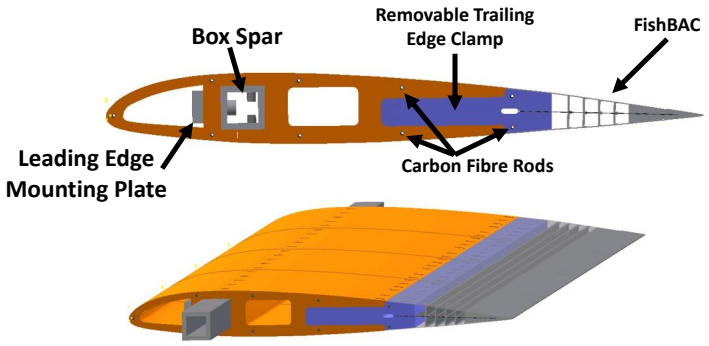


**Figure 4.** Profile view of the FishBAC wind tunnel model. Note that the tendons are missing in this CAD model.

### 3.2.2 Manufacture

The metal parts of the wind tunnel model (i.e. box spar, leading edge plate and torque transmission pulleys) are machined, while the main sections of the wing will be 3D-printed using an "ABS type" UV cured plastic. Furthermore, the FishBAC's spine was manufactured by hand layup, using Hexcel® 8552/IM7 carbon fibre prepreg (Figure 5). The carbon fibre was cured by vacuum bagging and autoclave at 180 °C with 6 bar of pressure. Lastly, the solid portions of the FishBAC's trailing edge and stringers will also be 3D-printed and then post-cured to the carbon spine. Lastly, the tendons will be made from Kevlar tape, while the actuators and carbon fibre pultrusions will be obtained off-the-shelf.

## 4. Conclusions

This paper introduces progress on the design, manufacture and wind tunnel test of a composite Fish Bone Active Camber (FishBAC) morphing wing. A two-dimensional discontinuous Kirchhoff-Love plate model has been developed to analyse the complex FishBAC structure, which is also capable to analyse fully anisotropic composite laminates. This new structural model is capable of capturing spanwise variations in static deformations.

The composite FishBAC spine has been sized based on actuation energy requirements needed to obtain a target tip deflections of 10% chord. The recently developed two-dimensional structural model has been baselined against a one-dimensional Euler-Bernoulli structural model, in absence of aerodynamic loads. Results show that both models agree within approximately 14%, when displacements along the spanwise free edge of the FishBAC are

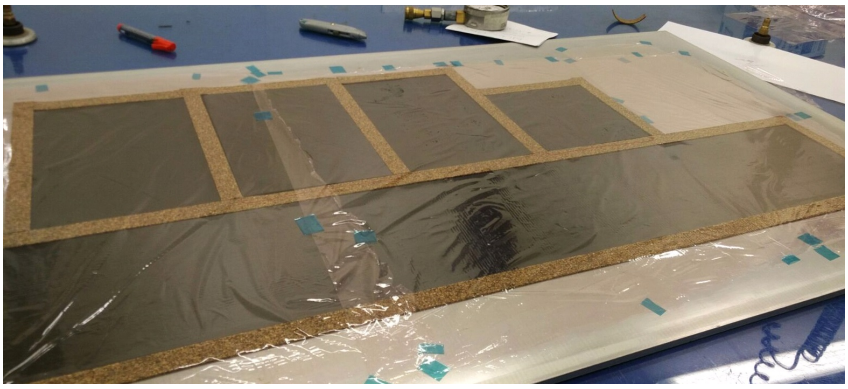

**Figure 5.** Hand layup and vacuum bagging of the composite spine and plates for material characterisation.

compared.

Furthermore, aerodynamic loads obtained using an already developed one-dimensional fluid-structure interaction model were applied to the two-dimensional plate model. This not only allows to select the actuators based on required actuation loads, but also allows to compare the deformations of the plate model with an already converged one-dimensional fluid-structure interaction model. Results show that the deflections under aerodynamic loads agree with each other within a mean percentage difference of 15%. Based on these results, it was decided that a $[90/0/90]$ carbon spine, with a total thickness of $0.375\,\mathrm{mm}$ will be used as the main load bearing member of the FishBAC.

Future work includes structural characterisation and wind tunnel testing of the composite FishBAC wing, for a wide range of flow speeds, angles of attack and FishBAC actuation inputs. Furthermore, a direct experimental wind tunnel comparison with a trailing edge plain flap will be performed, allowing for highlighting the benefits of active camber. Lastly, a fluid-structure interaction model will be developed around the two-dimensional discontinuous plate model. The model must be capable of obtaining both chordwise and spanwise aerodynamic pressure distributions, which would potentially allow for optimising spanwise lift distributions.

## ACKNOWLEDGEMENTS

This work was supported by the Engineering and Physical Sciences Research Council through the EPSRC Centre for Doctoral Training in Advanced Composites for Innovation and Science [grant number EP/L016028/1]. Furthermore, this project has received funding from the European Union's Horizon 2020 research and innovation programme under grant agreement No. 723491.

The second author would like to acknowledge the Royal Society for the Royal Society Wolfson Merit award and also the Science Foundation Ireland for the award of a Research Professor grant. The third author would like to acknowledge the Royal Academy of Engineering for the Research Professorship award.

## REFERENCES

[1] Y. Kovo, "Green aviation - improved aerodynamic efficiency and less fuel burn," 2015.

[2] H. Parker, "The Parker Variable Camber," Tech. Rep. 77, National Advisory Committee for Aeronautics, Washington, DC, 1920.

[3] H. J. Hogan, "Variable Camber Airfoil," 1932. US Patent 1,868,748.

[4] C. H. Grant, "Variable Camber Wing," 1939. US Patent 2,146,014.

[5] R. Chilton, "Variable Area-and-Camber Wing," 1940. US Patent 2,222,935.

[6] C. Thill, J. Etches, I. Bond, K. Potter, and P. Weaver, "Morphing skins," *Aeronaut. J.*, vol. 112, no. 1129, pp. 117–139, 2008.

[7] S. Barbarino, O. Bilgen, R. M. Ajaj, M. I. Friswell, and D. J. Inman, "A Review of Morphing Aircraft," *J. Intell. Mater. Syst. Struct.*, vol. 22, no. 9, pp. 823–877, 2011.

[8] J. N. Kudva, "Overview of the DARPA Smart Wing Project," *J. Intell. Mater. Syst. Struct.*, vol. 15, no. 4, pp. 261–267, 2004.

[9] S. Vasista, J. Riemenschneider, B. van de Kamp, H. P. Monner, R. C. M. Cheung, C. Wales, and J. E. Cooper, "Evaluation of a Compliant Droop-Nose Morphing Wing Tip via Experimental Tests," *J. Aircr.*, vol. 54, no. 2, pp. 519–534, 2017.

[10] A. De Gaspari, S. Ricci, and L. Riccobene, "Design, Manufacturing and Wind Tunnel Validation of an Active Camber Morphing Wing Based on Compliant Structures," *25th Int. Conf. Adapt. Struct. Technol. (ICAST 2014)*, no. January, pp. 1–12, 2014.

[11] O. Bilgen, M. I. Friswell, K. B. Kochersberger, and D. J. Inman, "Surface Actuated Variable-Camber and Variable-Twist Morphing Wings Using Piezocomposites," *Struct. Struct. Dyn. Mater. Conf.*, vol. 19, no. April, pp. 1–13, 2011.

[12] G. Molinari, M. Quack, V. Dmitriev, M. Morari, P. Jenny, and P. Ermanni, "Aero-Structural Optimization of Morphing Airfoils for Adaptive Wings," *J. Intell. Mater. Syst. Struct.*, vol. 22, no. 10, pp. 1075–1089, 2011.

[13] C. G. Diaconu, P. M. Weaver, and F. Mattioni, "Concepts for morphing airfoil sections using bi-stable laminated composite structures," *Thin-Walled Struct.*, vol. 46, no. 6, pp. 689–701, 2008.

[14] S. Daynes, S. Nall, P. Weaver, K. Potter, P. Margaris, and P. Mellor, "Bistable Composite Flap for an Airfoil," *J. Aircr.*, vol. 47, no. 1, pp. 334–338, 2010.

[15] B. A. Grohmann, C. Maucher, T. Prunhuber, P. Janker, O. Dieterich, B. Enenkl, M. Bauer, E. Ahci, A. Altmikus, and H. Baier, "Multidisciplinary design and optimization of active trailing edge for smart helicopter rotor blade," *Mech. Adv. Mater. Struct.*, vol. 15, no. 3-4, pp. 307–324, 2008.

[16] S. Barbarino, R. Pecora, L. Lecce, A. Concilio, S. Ameduri, and E. Calvi, "A novel SMA-based concept for airfoil structural morphing," *J. Mater. Eng. Perform.*, vol. 18, no. 5-6, pp. 696–705, 2009.

[17] F. Previtali, G. Molinari, A. F. Arrieta, M. Guillaume, and P. Ermanni, "Design and experimental characterisation of a morphing wing with enhanced corrugated skin," *J. Intell. Mater. Syst. Struct.*, vol. 27, no. 2, pp. 1–15, 2015.

[18] A. P. Milojević and N. D. Pavlović, "Development of a new adaptive shape morphing compliant structure with embedded actuators," *J. Intell. Mater. Syst. Struct.*, vol. 27, no. 10, pp. 1306–1328, 2016.

[19] N. Nguyen, K. Trinh, K. Reynolds, J. Kless, M. Aftosmis, J. Urnes, Sr., and C. Ippolito, "Elastically Shaped Wing Optimization and Aircraft Concept for Improved Cruise Efficiency," no. January, pp. 1–44, 2013.

[20] Flexsys, "flexfoil Variable Gemoetry Control Surfaces," 2014.

[21] B. K. S. Woods, "Pneumatic Artificial Muscle Driven Trailing Edge Flaps For Active Rotors," *ProQuest Diss. Theses*, vol. 3517579, p. 358, 2012.

[22] B. K. S. Woods and M. I. Friswell, "Structural Characterization of the Fish Bone Active Camber Morphing Airfoil," *22nd AIAA/ASME/AHS Adapt. Struct. Conf. AIAA SciTech*, no. January, 2014.

[23] B. K. Woods and M. I. Friswell, "Fluid-Structure Interaction Analysis of the Fish Bone Active Camber Mechanism," in *54th AIAA/ASME/ASCE/AHS/ASC Struct. Struct. Dyn. Mater. Conf.*, (Boston, Massachusetts), pp. 1–15, 2013.

[24] J. M. Whitney, *Structural Analysis of Laminated Anisotropic Plates*. Lancaster, Pennsylvania: Technomic Publishing, 1987.

[25] M. H. Hyer, *Stress Analysis of Fiber-Reinforced Composite Materials*. New Delhi: McGraw-Hill, 2014.

[26] E. H. Mansfield, *The Bending and Stretching of Plates*. Cambridge University Press, second ed., 1989.

[27] B. H. Coburn, Z. Wu, and P. M. Weaver, "Buckling analysis of stiffened variable angle tow panels," *Compos. Struct.*, vol. 111, no. 1, pp. 259–270, 2014.

[28] R. Vescovini and C. Bisagni, "Buckling analysis and optimization of stiffened composite flat and curved panels," *AIAA J.*, vol. 50, no. 4, pp. 904–915, 2012.

[29] Z. Wu, G. Raju, and P. M. Weaver, "Comparison of Variational, Differential Quadrature, and Approximate Closed-Form Solution Methods for Buckling of Highly Flexurally Anisotropic Laminates," *J. Eng. Mech.*, vol. 139, no. 8, pp. 1073–1083, 2012.

[30] S. Ilanko, L. Monterrubio, and Y. Mochida, *The Rayleigh-Ritz Method for Structural Analysis*. Iste Series, London and New York: Wiley, 2015.

[31] B. H. Coburn, *Buckling of stiffened variable stiffness panels*. PhD Thesis, University of Bristol, 2015.

[32] H. Richard and M. Raffel, "Rotor wake measurements: Full-scale and model tests.," in *58th Annu. Forum Am. Helicopter Soc.*, (Montreal, Canada), pp. 1–9, 2002.

[33] Cambridge University Engineering Department, "Materials Data Book," Cambridge University, Cambridge, UK, 2003.

[34] KST, "X10 Wing Servo," *Tech. Specif.*, pp. 2–5, 2017.